Electronic Supplementary Information

Membrane interaction and selectivity of novel alternating cationic lipid-nanodisc assembling polymers

Michelle D. Farrelly[a], Jiali Zhai[b], Alice Y.J. Tiong[c], Leonie van 't Hag[c], Heidi H. Yu[d], Jian Li[d], Lisandra L. Martin[a]*, San H. Thang[a]*

[a] School of Chemistry, Monash University, Clayton, VIC 3800 Australia.

[b] School of Science, STEM College, RMIT University, Melbourne, VIC 3000 Australia.

[c] Department of Chemical and Biological Engineering, Monash University, Clayton, VIC 3800 Australia.

[d] Infection Program and Department of Microbiology, Biomedicine Discovery Institute, Monash University, Clayton, VIC 3800 Australia.

Corresponding Authors: Lisa.Martin@monash.edu, San.Thang@monash.edu

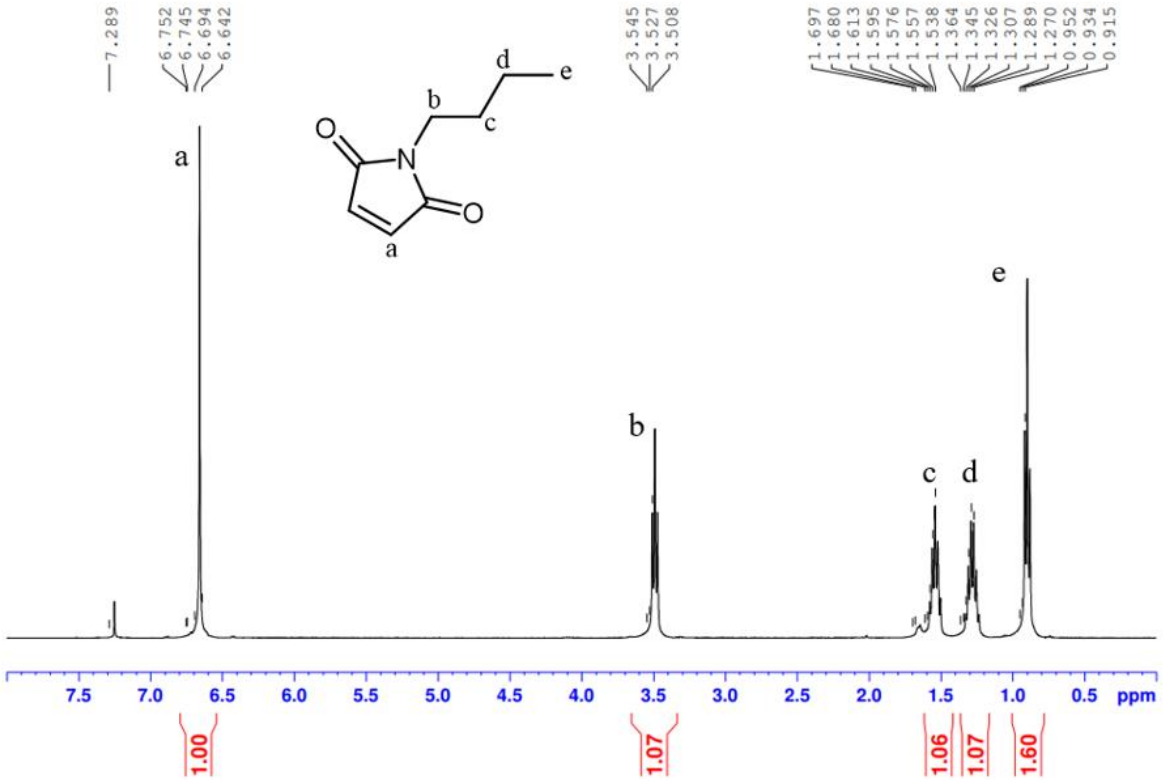

Figure S1. ^{1}H NMR spectrum of *N*-*n*-butyl maleimide monomer. ^{1}H NMR ($CDCl_3$, 400 MHz): δ(ppm) 0.93 (t, 3H, J =7.4 Hz), 1.33 (m, 2H, J =7.6 Hz), 1.58 (m, 2H, J =7.6 Hz), 3.53 (t, 2H, J =7.4 Hz), 6.70 (s, 2H).

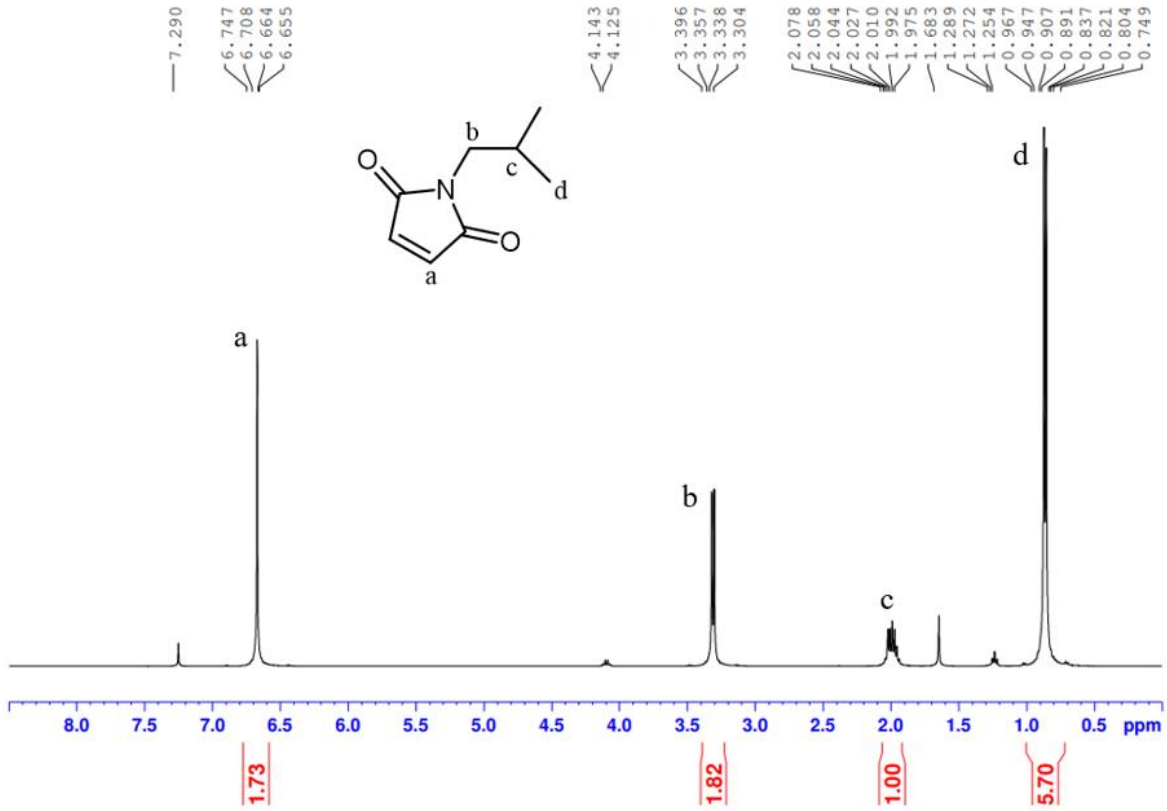

Figure S2. ^{1}H NMR spectrum of *N-iso*-butyl maleimide monomer. ^{1}H NMR ($CDCl_3$, 400 MHz): δ(ppm) 0.90 (d, 6H, J = 6.4 Hz), 2.03 (m, 1H, J = 6.4, 7.6 Hz), 3.36 (d, 2H, J = 7.6 Hz), 6.70 (s, 2H).

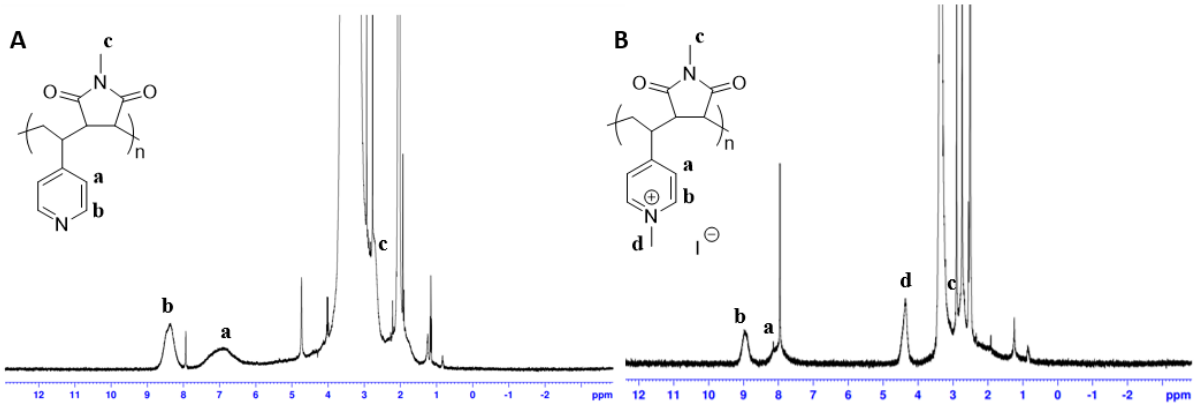

Figure S3. ^{1}H NMR spectra validating the quaternisation process converting **(A)** poly(4-vinyl pyridine-*co*-*N*-methylmaleimide) into **(B)** poly(*N*-methyl-4-vinyl pyridinium iodide-*co*-N-methylmaleimide).

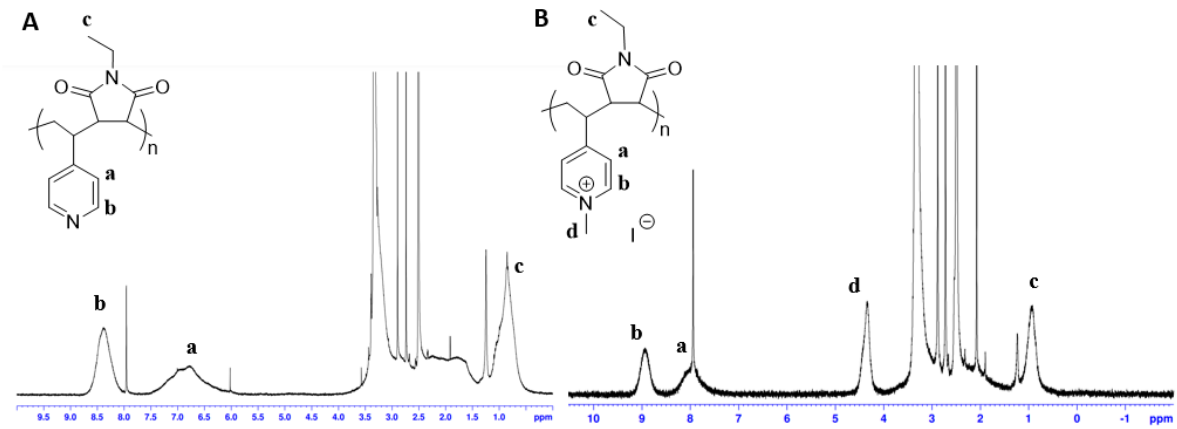

Figure S4. ^{1}H NMR spectra validating the quaternisation process converting **(A)** poly(4-vinyl pyridine-*co*-*N*-ethylmaleimide) into **(B)** poly(*N*-methyl-4-vinyl pyridinium iodide-*co*-*N*-ethylmaleimide).

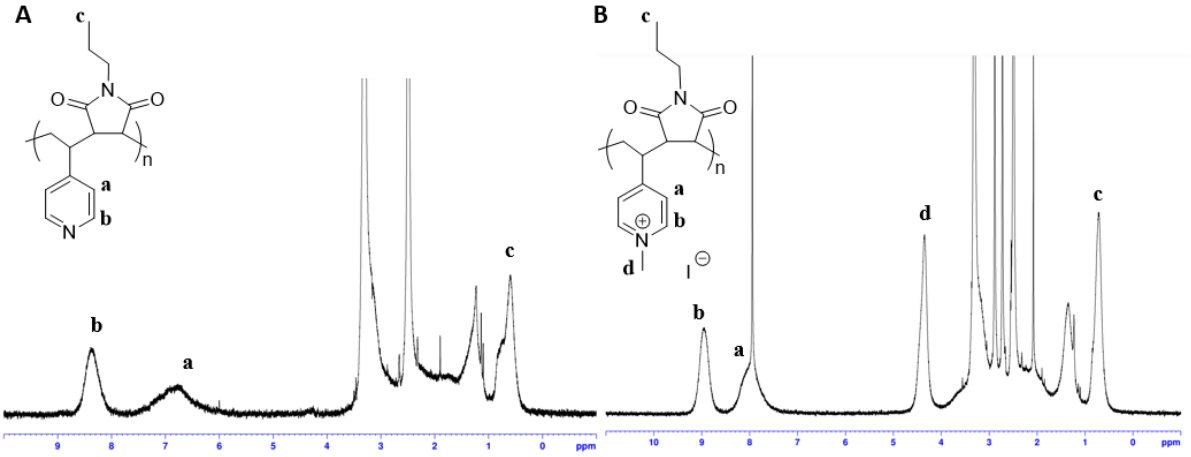

Figure S5. ^{1}H NMR spectra validating the quaternisation process converting **(A)** poly(4-vinyl pyridine-*co*-*N*-*n*-propylmaleimide) into **(B)** poly(*N*-methyl-4-vinyl pyridinium iodide-*co*-*N*-*n*-propylmaleimide).

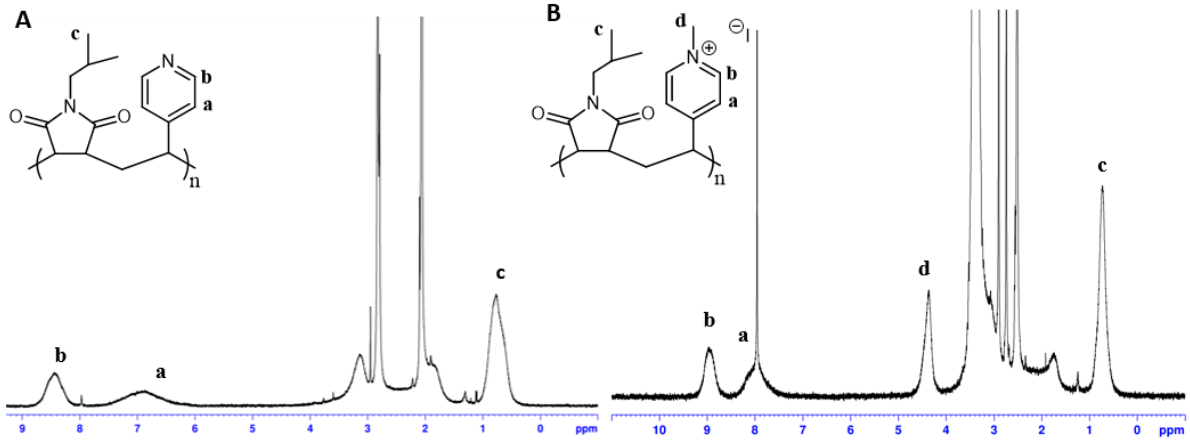

Figure S6. ^{1}H NMR spectra validating the quaternisation process converting **(A)** poly(4-vinyl pyridine-*co*-*N*-*iso*-butylmaleimide) into **(B)** poly(*N*-methyl-4-vinyl pyridinium iodide-*co*-*N*-*iso*-butylmaleimide).

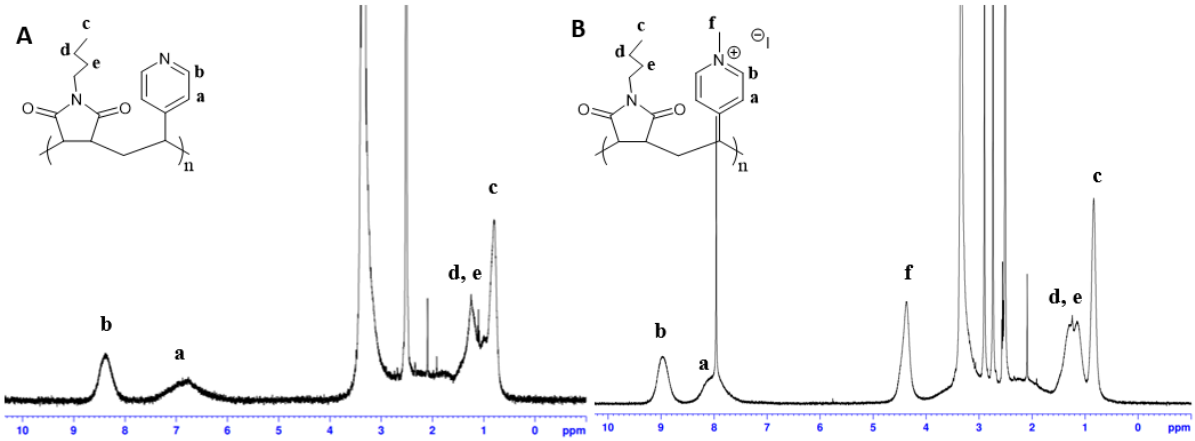

Figure S7. ^{1}H NMR spectra validating the quaternisation process converting **(A)** poly(4-vinyl pyridine-*co*-*N*-*n*-butylmaleimide) into **(B)** poly(*N*-methyl-4-vinyl pyridinium iodide-*co*-*N*-*n*-butylmaleimide).

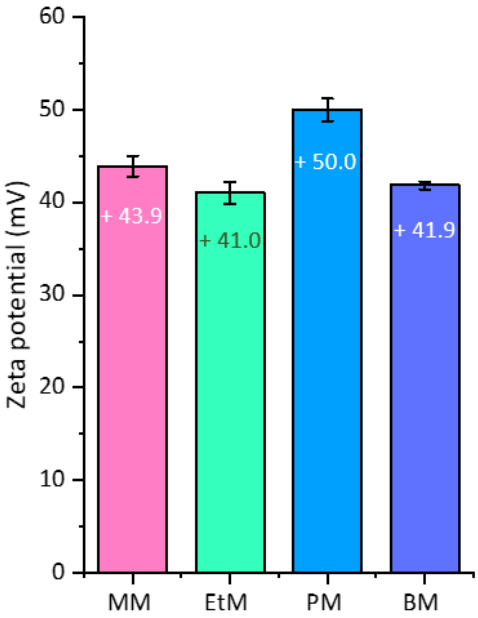

Figure S8. Average zeta potential measurements for 0.625 mM poly(MVP-*co*-MM) (MM), poly(MVP-*co*-EtM) (EtM), poly(MVP-*co*-PM) (PM) and poly(MVP-*co*-BM) (BM) dissolved in Milli-Q® water. Error bars signify the mean standard deviation of the zeta potential distribution function.

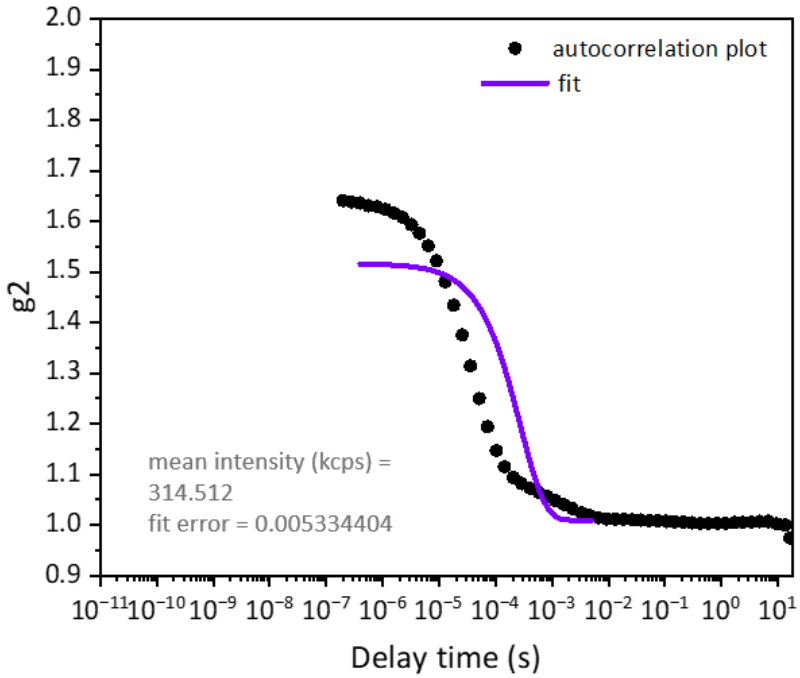

Figure S9. Fitted autocorrelation function for DLS measurement of poly(MVP-*co*-BM) added to DMPC LUVs at 0.1:1 polymer:lipid

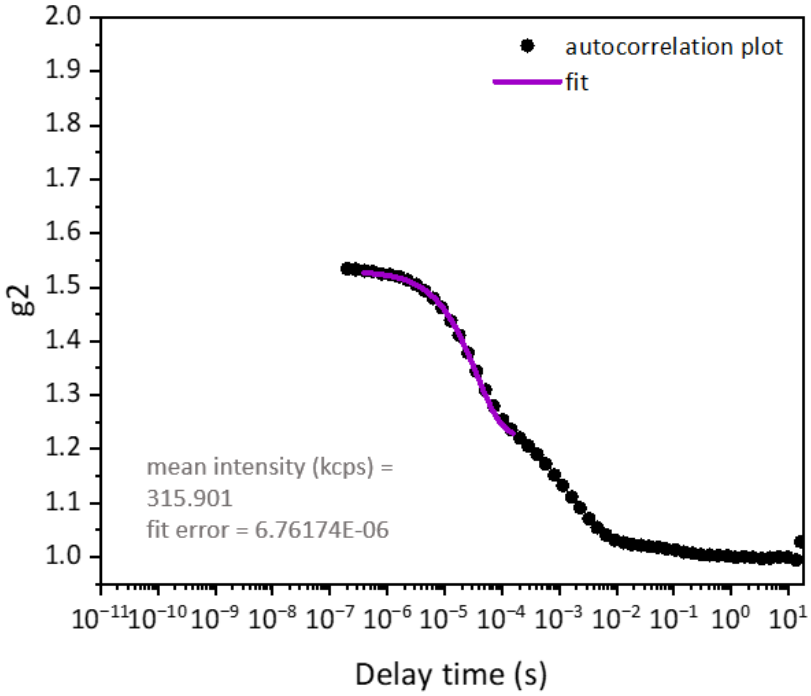

Figure S10. Fitted autocorrelation function for DLS measurement of poly(MVP-*co*-BM) added to DMPC LUVs at 0.2:1 polymer:lipid.

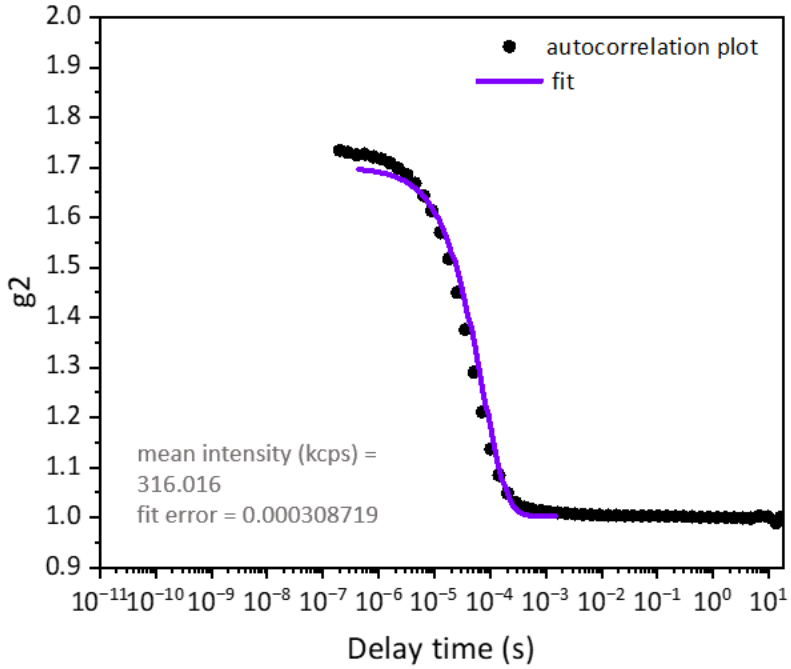

Figure S11. Fitted autocorrelation function for DLS measurement of poly(MVP-*co*-IBM) added to DMPC LUVs at 0.1:1 polymer:lipid.

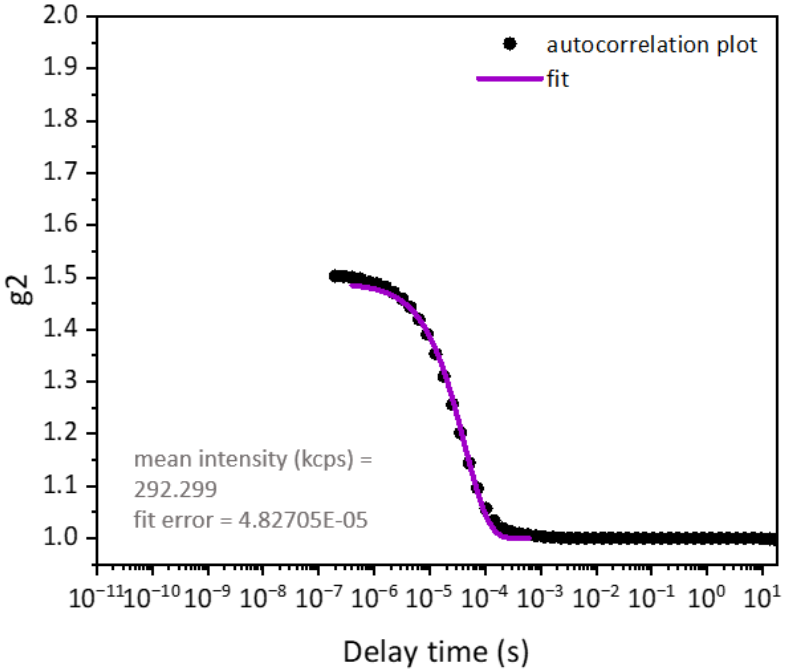

Figure S12. Fitted autocorrelation function for DLS measurement of poly(MVP-*co*-IBM) added to DMPC LUVs at 0.2:1 polymer:lipid.

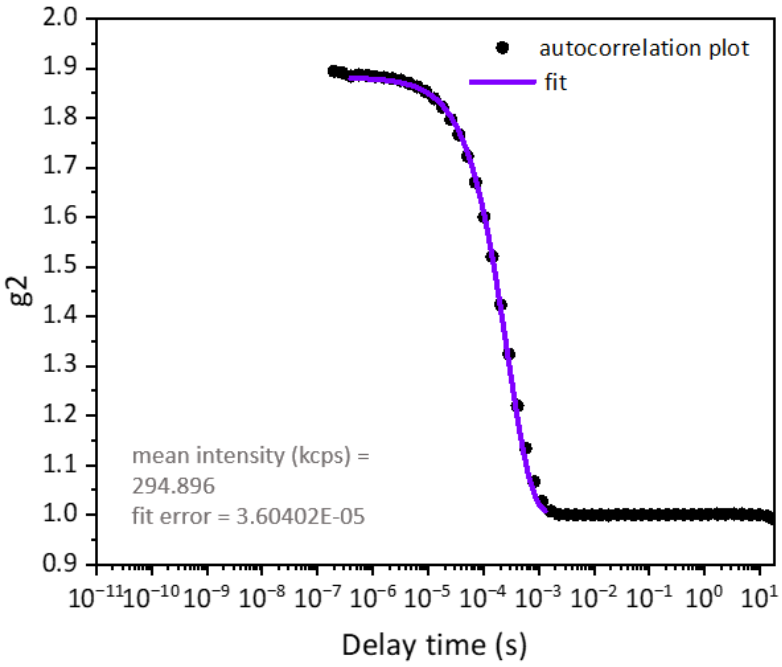

Figure S13. Fitted autocorrelation function for DLS measurement of poly(MVP-*co*-PM) added to DMPC LUVs at 0.1:1 polymer:lipid.

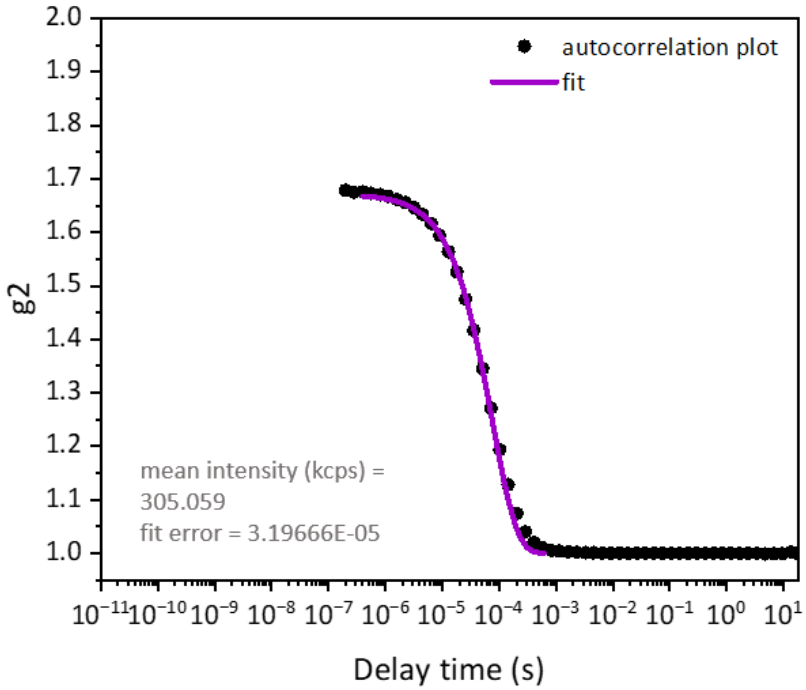

Figure S14. Fitted autocorrelation function for DLS measurement of poly(MVP-*co*-PM) added to DMPC LUVs at 0.2:1 polymer:lipid.

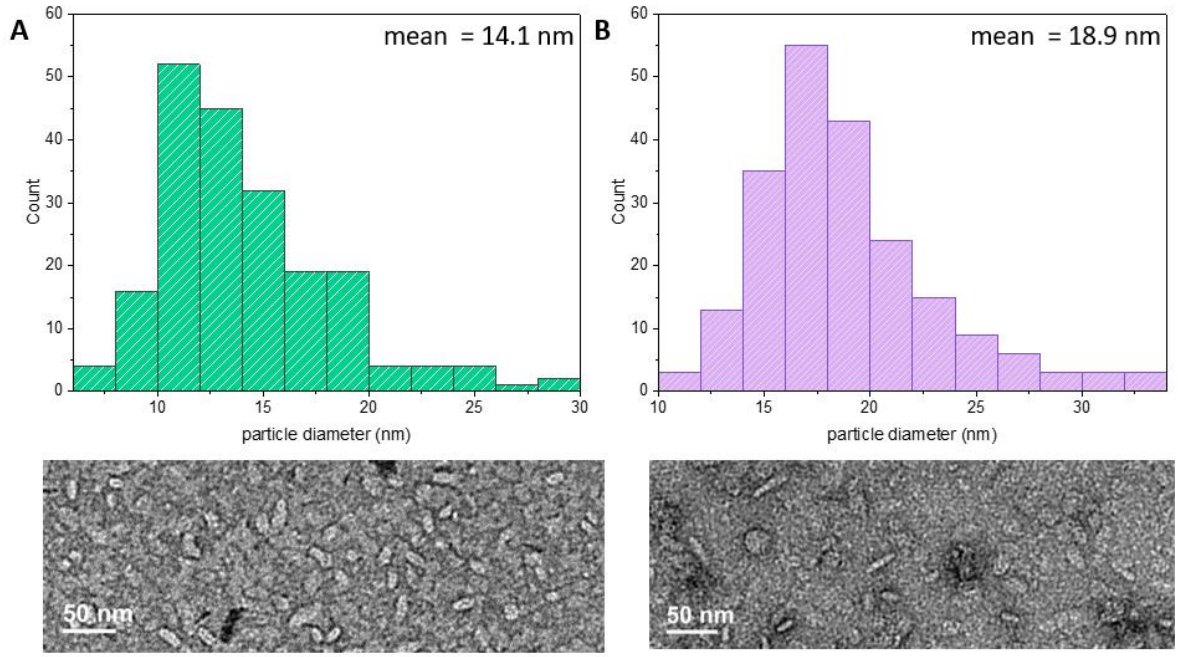

Figure S15. TEM derived histograms (constructed using imageJ analysis of at least 100 particles across two different axes) and accompanying images for poly(MVP-*co*-BM) added to DMPC LUVs in **(A)** 0.2:1 polymer:lipid and **(B)** 0.1:1 polymer:lipid ratios.

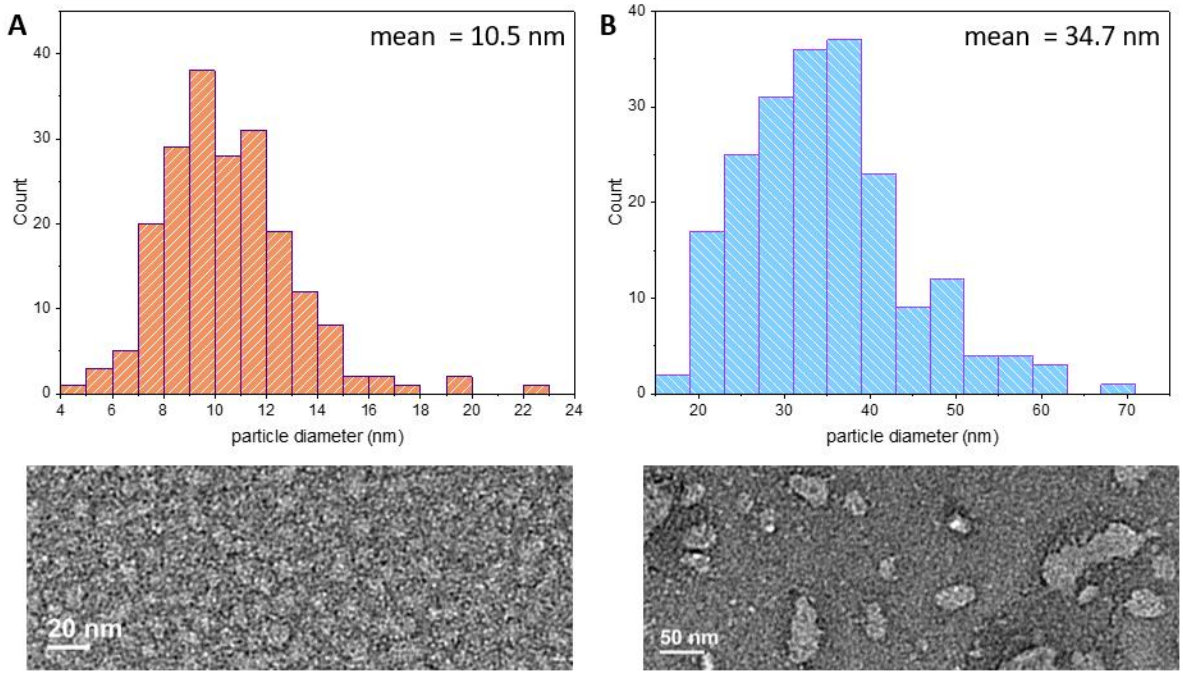

Figure S16. TEM derived histograms (constructed using imageJ analysis of at least 100 particles across two different axes) and accompanying images for poly(MVP-*co*-IBM) added to DMPC LUVs in **(A)** 0.2:1 polymer:lipid and (B) 0.1:1 polymer:lipid ratios.

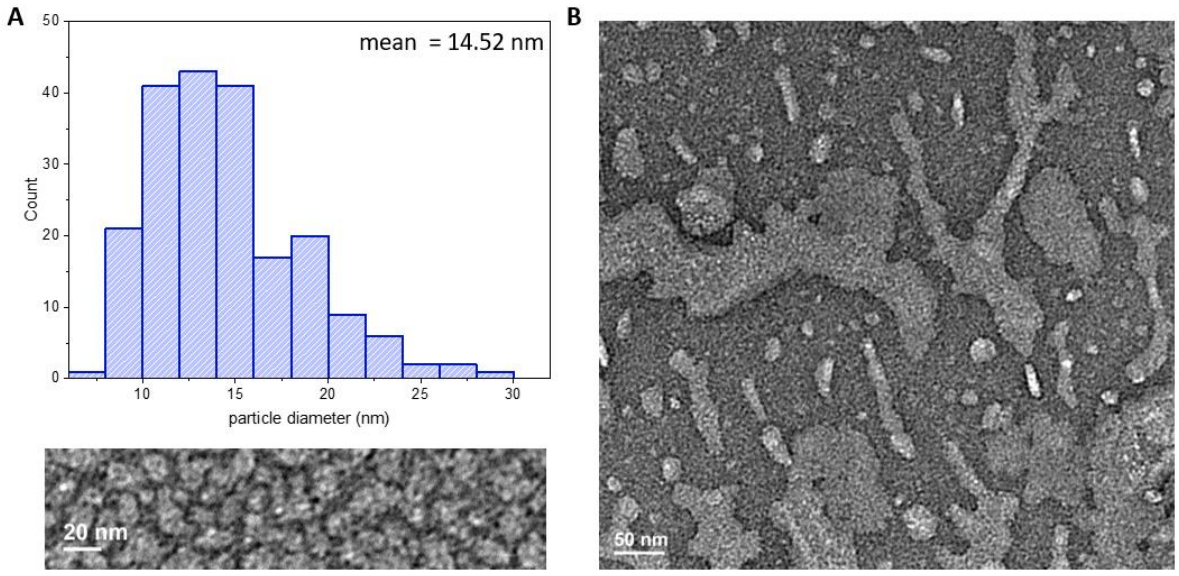

Figure S17. (A) TEM derived histogram (constructed using imageJ analysis of at least 100 particles across two different axes) and accompanying images for poly(MVP-*co*-PM) added to DMPC LUVs in a 0.2:1 polymer:lipid ratio and **(B)** TEM image of poly(MVP-*co*-PM) added to DMPC LUVs in a 0.1:1 polymer:lipid ratio.

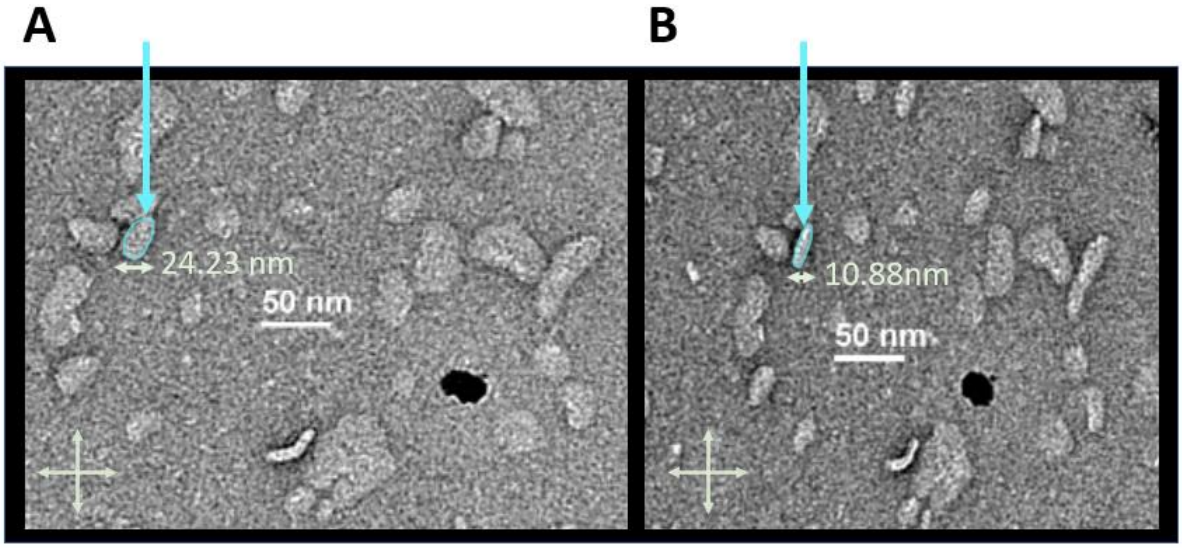

Figure S18. Comparison between TEM image of poly(MVP-*co*-IBM) added to DMPC 0.1:1 polymer: lipid at **(A)** 0 degrees sample stage α-tilt and at **(B)** 50 degrees sample stage α-tilt. The same particle has been measured along the horizontal axis as 24.23 nm at 0 degrees α-tilt and 10.88 nm at 50 degrees α-tilt.

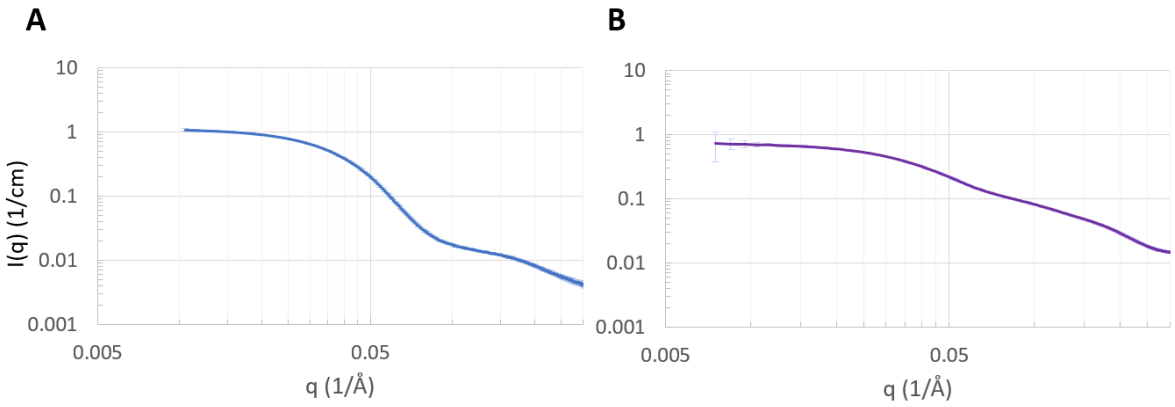

Figure S19. SAXS I(q) versus q plots for **(A)** diblock SMA (D10) and **(B)** poly(MVP-*co*-BM) polymer only controls with a polymer concentration of 1.1 mM in aqueous buffer.

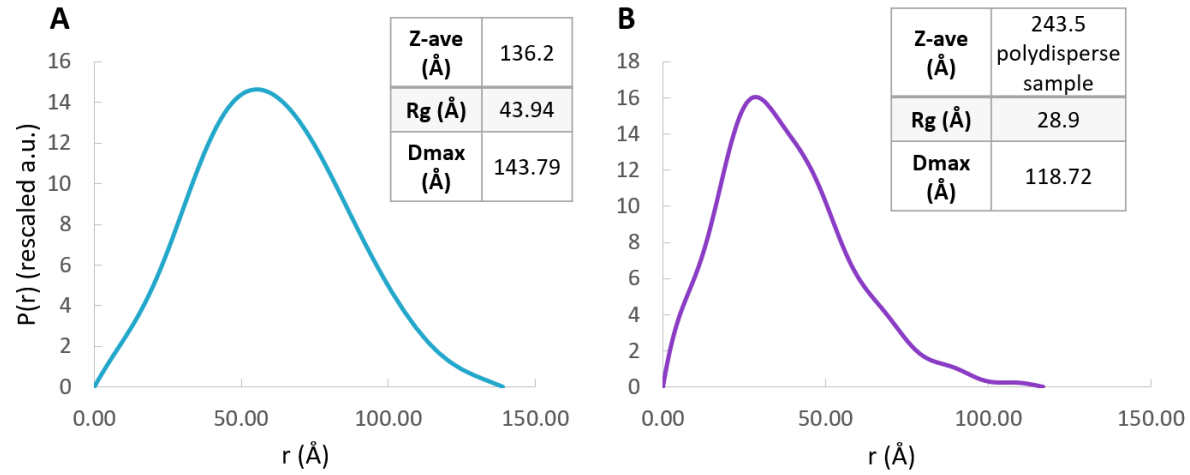

Figure S20. P(r) functions generated from SAXS of **(A)** diblock SMA (D10) and **(B)** poly(MVP-*co*-BM) polymer only controls at a concentration of 1.1 mM polymer. Zeta average diameter (Z-Ave) was collected from DLS, radius of gyration (Rg) was extracted from Guinier analysis of SAXS data and Dmax was given by the P(r) function intercept.

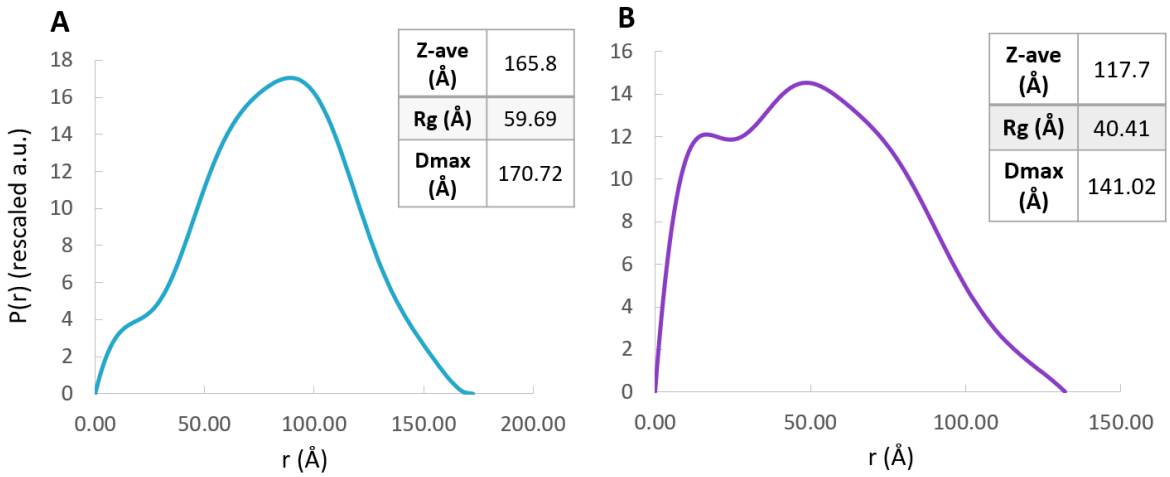

Figure S21. P(r) functions generated from SAXS of **(A)** diblock SMA (D10) added to DMPC LUVs (0.2:1 polymer to DMPC) at DMPC concentration of 5.6mM and polymer concentration of 1.1 mM (C1) and **(B)** poly(MVP-*co*-BM) added to DMPC LUVs (0.2:1 polymer to DMPC) at C1. Zeta average diameter (Z-Ave) was collected from DLS, radius of gyration (Rg) was extracted from Guinear analysis of SAXS data and Dmax was given by the P(r) function intercept.

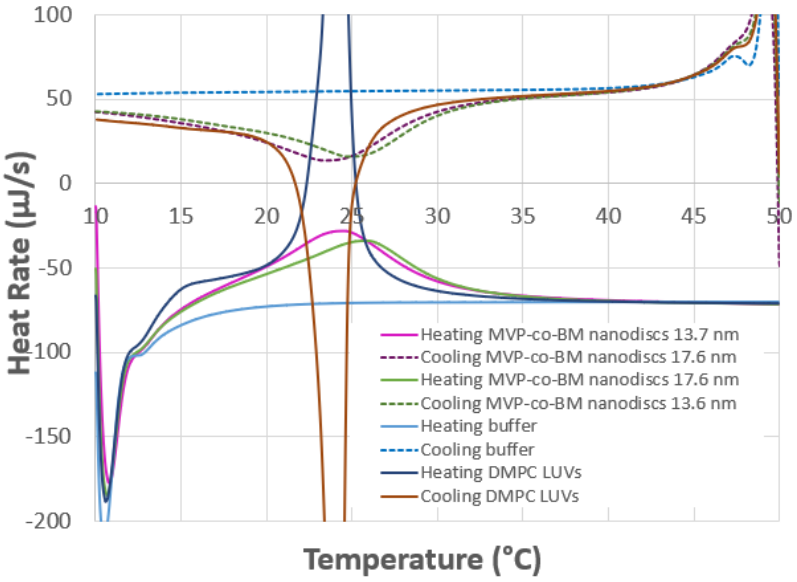

Figure S22. Raw DSC thermograms for both heating and cooling cycles showing the heat rate (µJ/s) of HS PBS buffer, 7.14 mM DMPC initially in the form of LUVs and upon incubation with a 0.2 molar fraction of poly(MVP-*co*-BM) polymer to form 13.7 nm and with a 0.1 molar fraction of poly(MVP-*co*-BM) to form 17.6 nm nanodiscs.

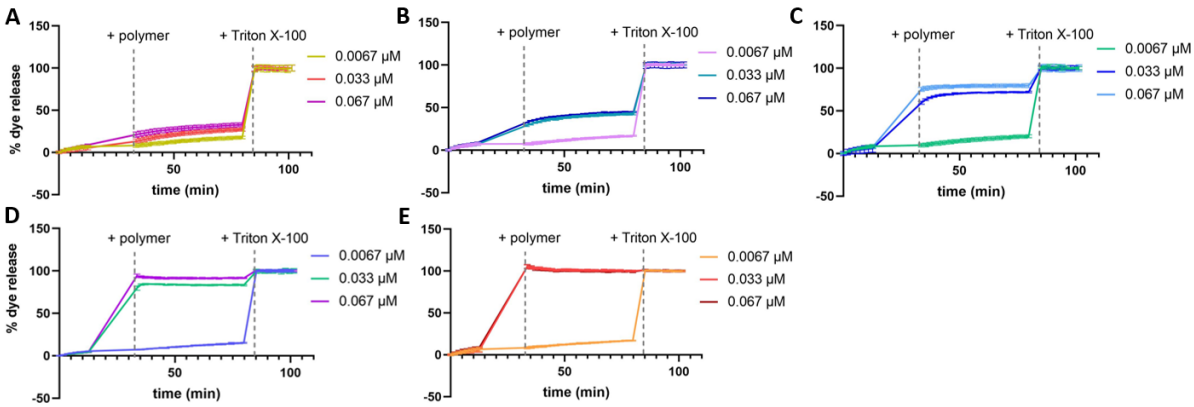

Figure S23. Normalised dye-release assay graphs measuring % dye-release over time from CF dye-loaded POPC LUVs after an initial polymer addition (across a concentration range from 0.0067 µM to 0.067 µM) of **(A)** poly(MVP-*co*-MM), **(B)** poly(MVP-*co*-EtM), **(C)** poly(MVP-*co*-PM), **(D)** poly(MVP-*co*-IBM) and **(E)** poly(MVP-*co*-BM) followed by a successive Triton X-100 addition to lyse any intact LUVs, thus indicating 100% dye-release.

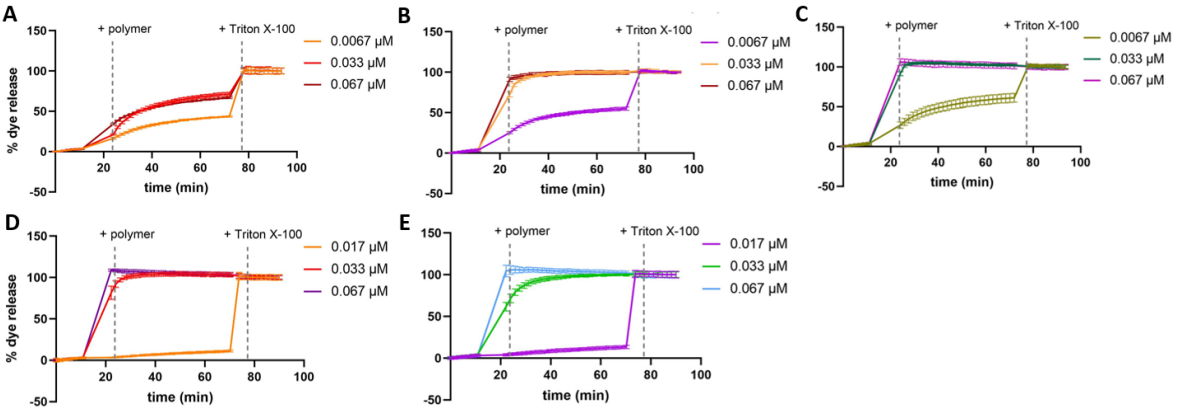

Figure S24. Normalised dye-release assay graphs measuring % dye-release over time from CF dye-loaded POPC:POPG (1:1) LUVs after an initial polymer addition (across a concentration range from 0.0067 µM to 0.067 µM) of **(A)** poly(MVP-*co*-MM), **(B)** poly(MVP-*co*-EtM), **(C)** poly(MVP-*co*-PM), **(D)** poly(MVP-*co*-IBM) and **(E)** poly(MVP-*co*-BM) followed by a successive Triton X-100 addition to lyse any intact LUVs thus indicating 100% dye-release.

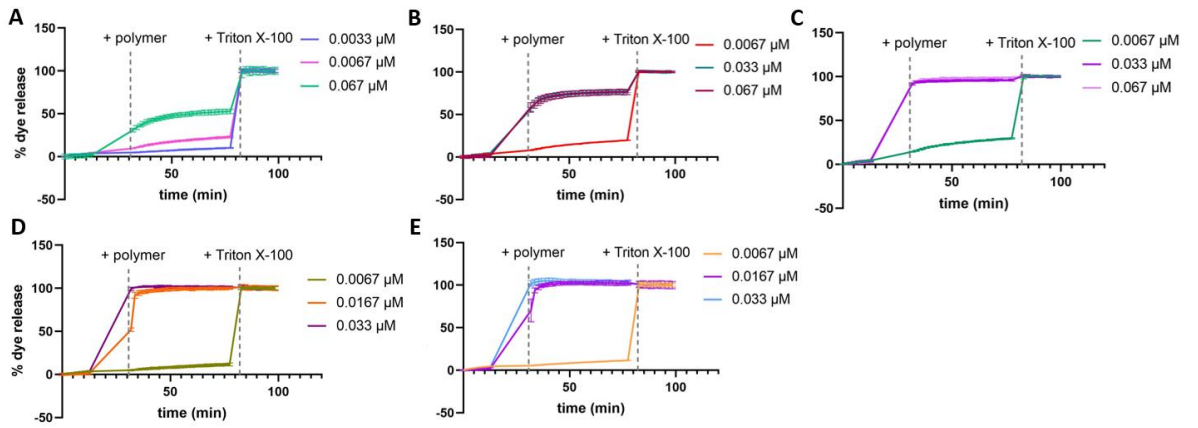

Figure S25. Normalised dye-release assay graphs measuring % dye-release over time from CF dye-loaded POPC:POPG (4:1) LUVs after an initial polymer addition (across a concentration range from 0.0067 μM to 0.067 μM) of **(A)** poly(MVP-*co*-MM), **(B)** poly(MVP-*co*-EtM), **(C)** poly(MVP-*co*-PM), **(D)** poly(MVP-*co*-IBM) and **(E)** poly(MVP-*co*-BM) followed by a successive Triton X-100 addition to lyse any intact LUVs thus indicating 100% dye-release.

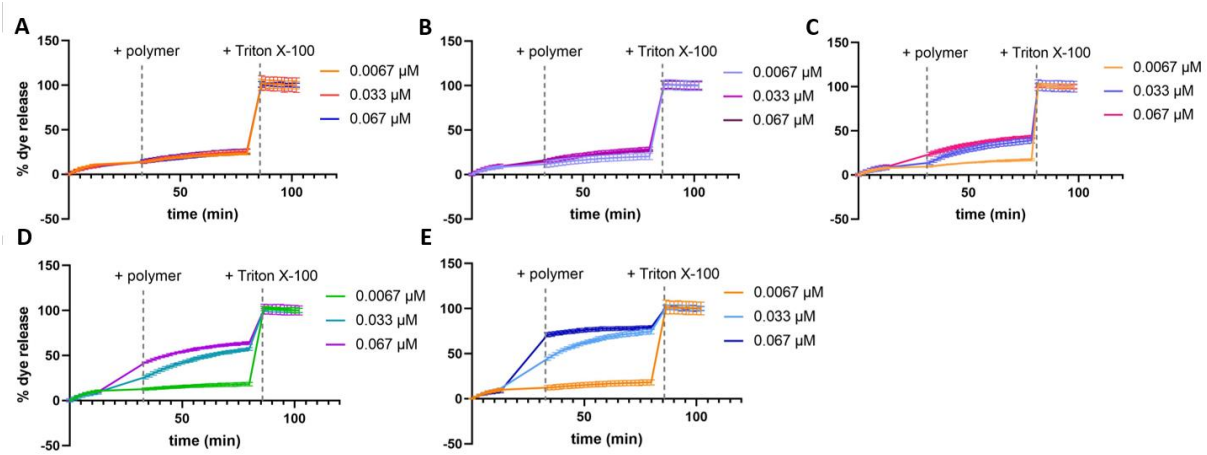

Figure S26. Normalised dye-release assay graphs measuring % dye-release over time from CF dye-loaded POPE:POPG:CL (15:4:1) LUVs after an initial polymer addition (across a concentration range from 0.0067 μM to 0.067 μM) of **(A)** poly(MVP-*co*-MM), **(B)** poly(MVP-*co*-EtM), **(C)** poly(MVP-*co*-PM), **(D)** poly(MVP-*co*-IBM) and **(E)** poly(MVP-*co*-BM) followed by a successive Triton X-100 addition to lyse any intact LUV s, thus indicating 100% dye-release.

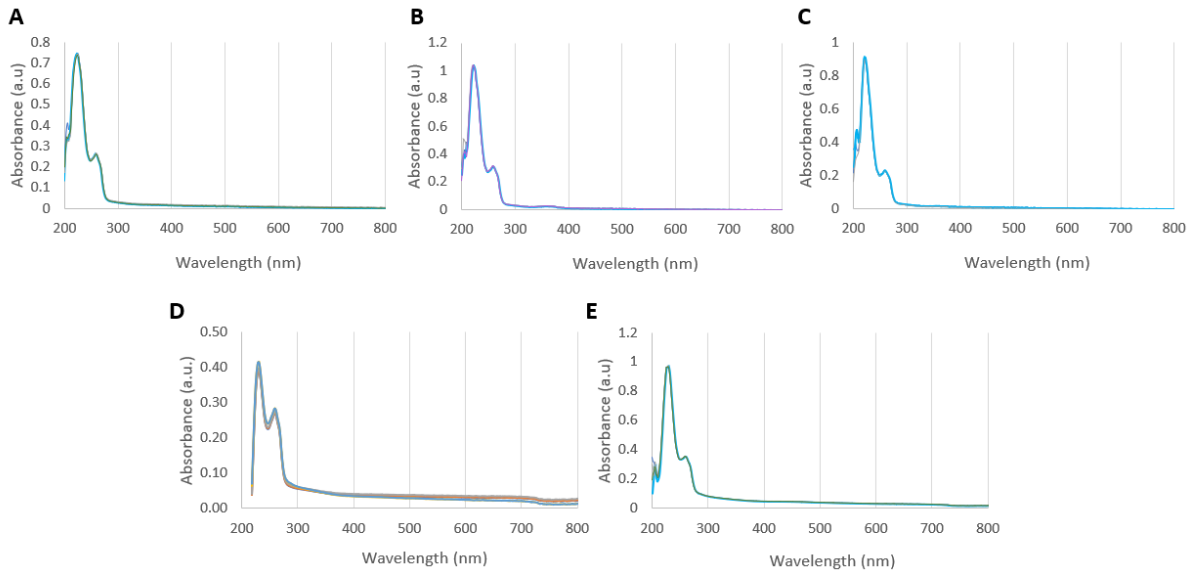

Figure S27. UV-vis absorption spectra of **(A)** poly(MVP-*co*-MM), **(B)** poly(MVP-*co*-EtM), **(C)** poly(MVP-*co*-PM), **(D)** poly(MVP-*co*-IBM), **(E)** poly(MVP-*co*-BM) in 1 x HEPES buffer.

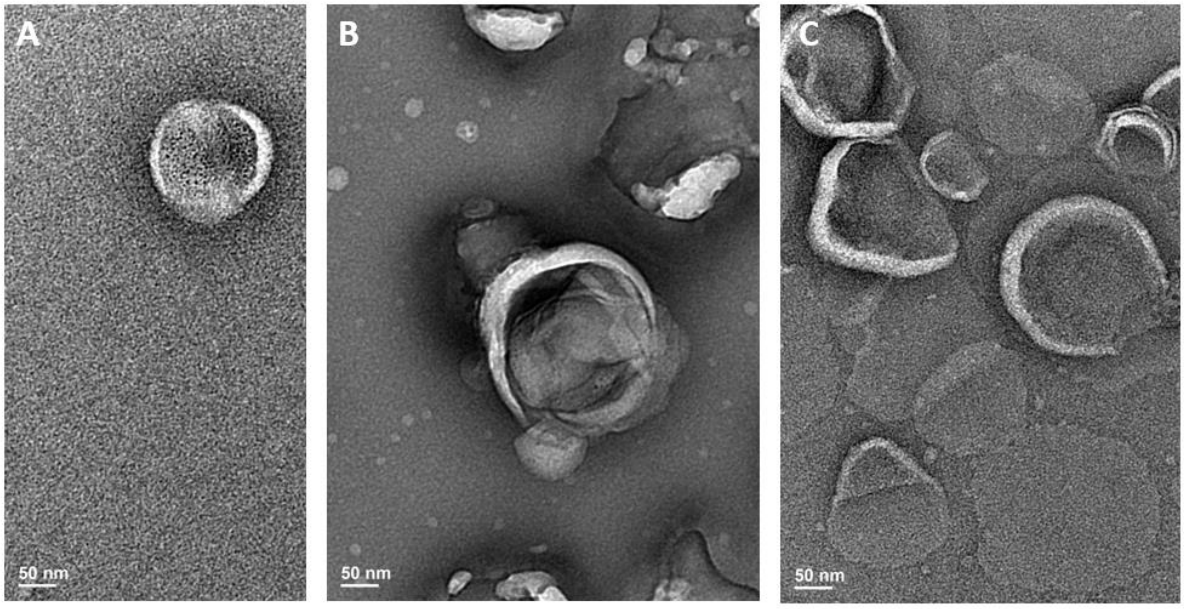

Figure S28. TEM images of **(A)** poly(MVP-*co*-MM), **(B)** poly(MVP-*co*-EtM) and **(C)** poly(MVP-*co*-PM) added to POPC:POPG (1:1) LUVs in a 0.2:1 polymer:lipid ratio.

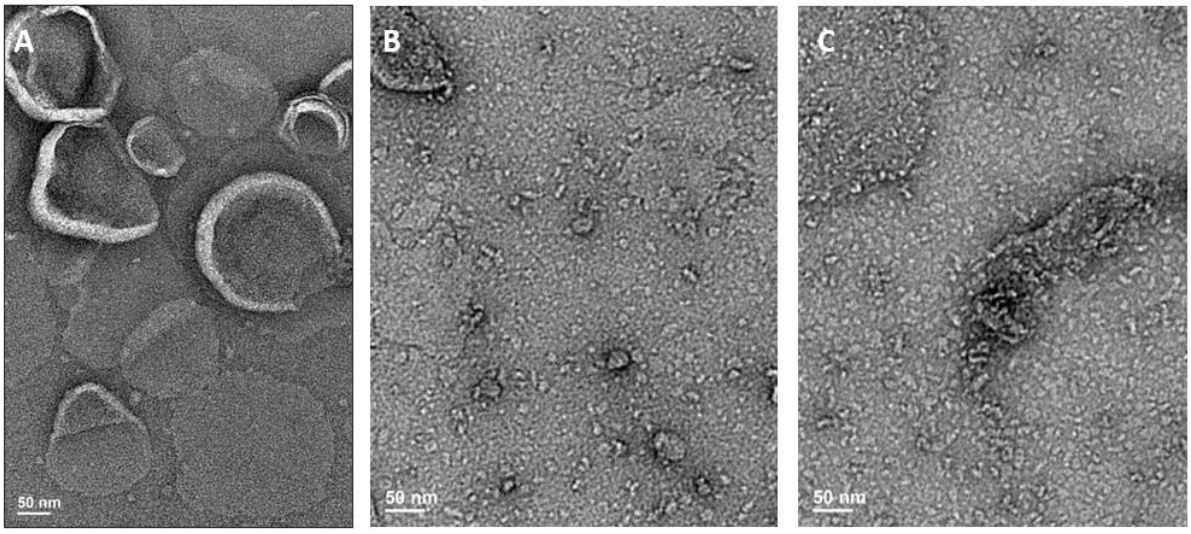

Figure S29. TEM images of **(A)** poly(MVP-*co*-PM), **(B)** poly(MVP-*co*-IBM) and **(C)** poly(MVP-*co*-BM) added to POPC:POPG (1:1) LUVs in a 0.2:1 polymer:lipid ratio.

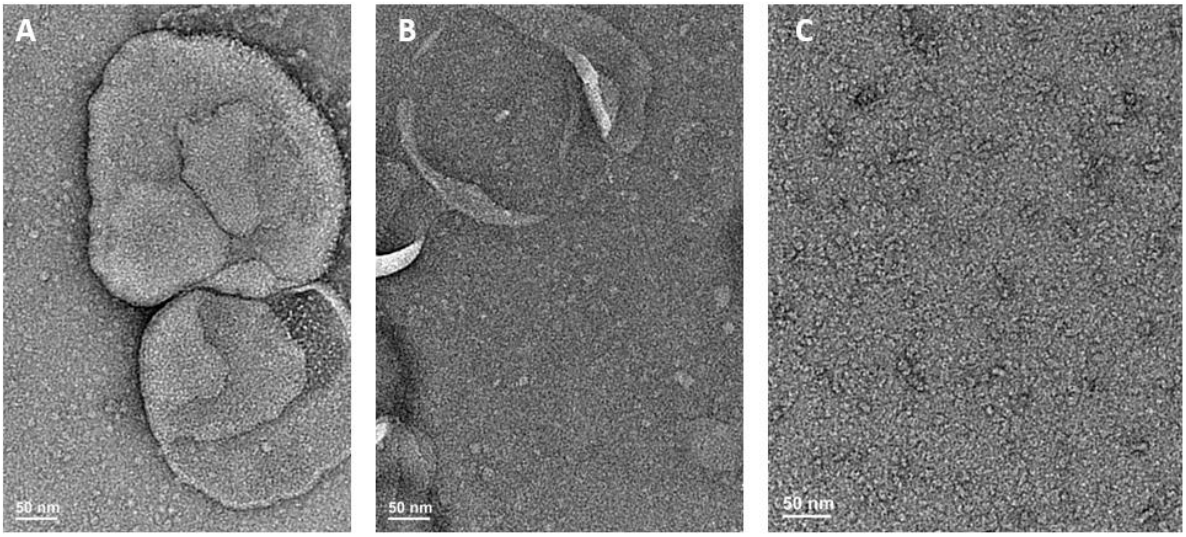

Figure S30. TEM images of **(A)** poly(MVP-*co*-PM), **(B)** poly(MVP-*co*-IBM) and **(C)** poly(MVP-*co*-BM) added to POPC LUVs in a 0.2:1 polymer:lipid ratio.

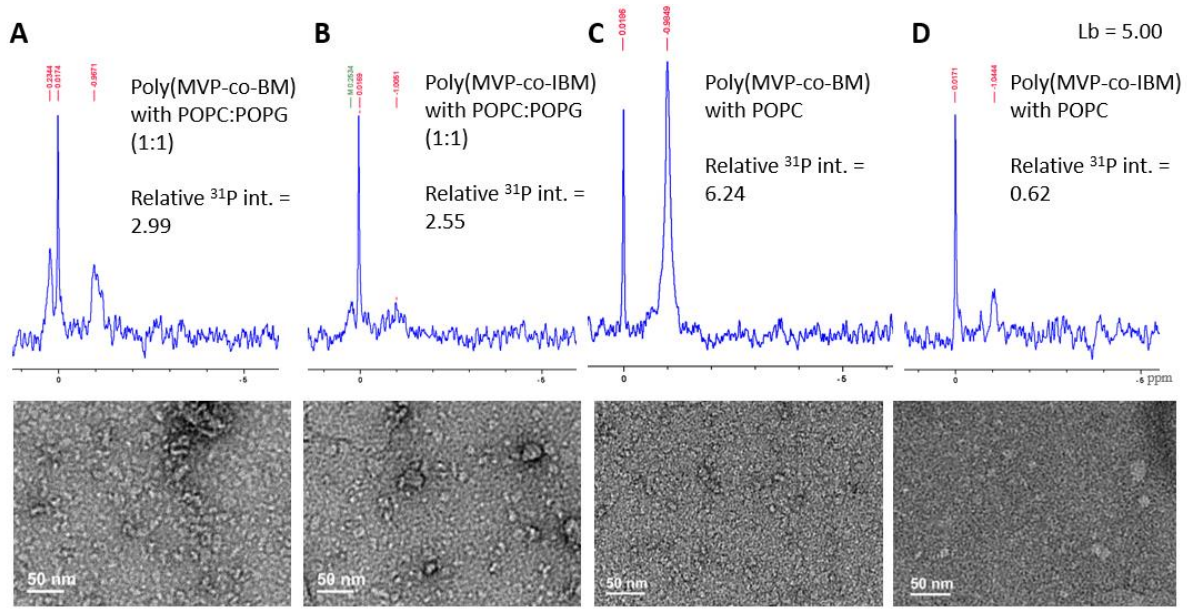

Figure S31. ^{31}P NMR spectra with accompanyingTEM images for comparison of **(A)** poly(MVP-*co*-PM) and **(B)** poly(MVP-*co*-IBM) added to POPC:POPG (1:1) LUVs in a 0.2:1 polymer to lipid ratio and **(C)** poly(MVP-*co*-BM) and **(D)** poly(MVP-*co*-IBM) added to POPC LUVs in a 0.2:1 polymer:lipid ratio. Relative ^{31}P integration was calculated as a ratio between the area under peaks assigned to phosphate lipid headgroups in nanodiscs (δ ~ 0.2 ppm for POPG and δ ~ - 1.0 ppm for POPC) and the H_3PO_4 external standard peak (δ ~ 0 ppm). NMR Data was multiplied by line broadening factor 5 (Lb = 5.00) before Fourier transformation.

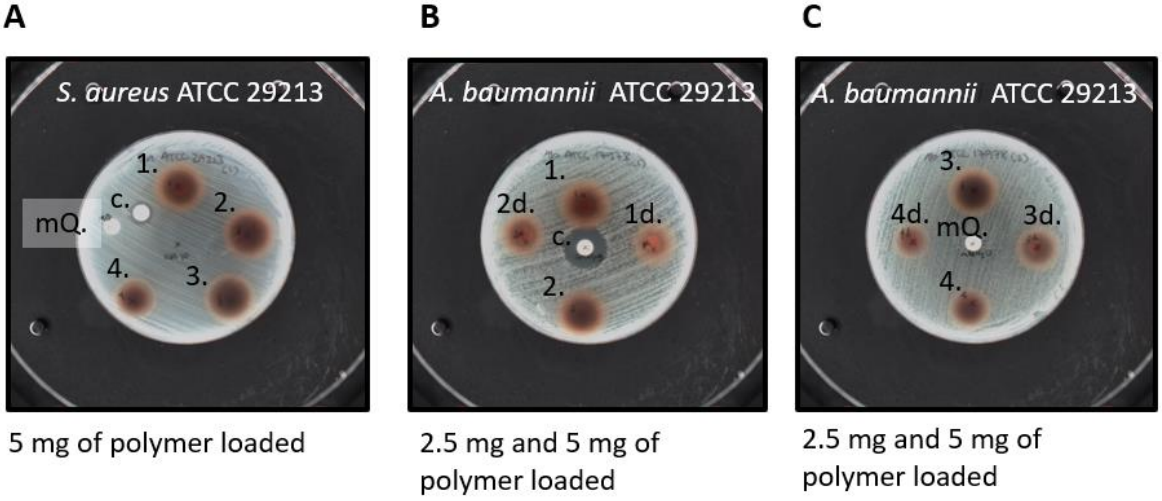

Figure S32. Disk diffusion assays of poly(MVP-*co*-MM) (1.), poly(MVP-*co*-EtM) (2.), poly(MVP-*co*-PM) (3.) and poly(MVP-*co*-BM) (4.) using 2.5 (indicated by 'd') or 5 mg of polymer loaded onto disks which were placed on agar plates incolucated with **(A)** *S. aureus* ATCC 29213 or **(B-C)** *A. baumannii* ATCC 29213. Positive control disks containing 10 µg colistin (c.) and negative control disks containing milliQ (mQ.) water are labelled.

Sample	polymer:lipid	TEM mean diameter (nm)	DLS H.D. (nm)	DLS peak # 1 diameter (int.)	DLS peak # 1 diameter (vol.)	DLS % PDI
Poly(MVP-*co*-BM) + DMPC	0.1:1	18.9	17.2	18.9	13.9	21.6
LUVs	0.2:1	14.1	23.0	12.5	10.1	20.0
Poly(MVP-*co*-IBM) + DMPC	0.1:1	34.7	42.0	31.9	21.7	18.3
LUVs	0.2:1	10.5	26.6	22.1	15.3	21.9
Poly(MVP-*co*-PM) + DMPC	0.1:1	-	163.2	33.8	23.2	20.7
LUVs	0.2:1	14.5	37.6	47.1	28.9	23.4

Table S1. TEM and DLS particle parameter summary for cationic polymers poly(MVP-*co*-BM), poly(MVP-*co*-IBM) and poly(MVP-*co*-PM) added to DMPC LUVs in 0.1:1 and 0.2:1 polymer:lipid molar ratios. Parameters shown are mean particle diameter (nm) calculated from TEM image analysis, DLS hydrodynamic diameter (H.D.) (nm), smallest particle fraction (peak # 1) diameter (nm) calculated from DLS intensity and volume weighted size frequency distributions and DLS percentage polydispersity index (% PDI).

	MIC (μg/mL)			
Strain ID	**Poly(MVP-*co*-MM)**	**Poly(MVP-*co*-EtM)**	**Poly(MVP-*co*-PM)**	**Poly(MVP-*co*-BM)**
***P. aeruginosa* ATCC 27853**	>1024	>1024	>1024	>1024
***A. baumannii* ATCC 17978**	>1024	>1024	1024	256
***S. aureus* ATCC 29213**	>1024	>1024	1024	256

Table S2. Minimal inhibitory concentrations (MIC) for poly(MVP-*co*-MM), poly(MVP-*co*-EtM), poly(MVP-*co*-PM) and poly(MVP-*co*-BM) polymers tested against *P. aeruginosa* ATCC 27853, *A. baumannii* ATCC 17978 and *S. aureus* ATCC 29213.